

Early Metal Mediated P–P Bond Formation in $\text{Cp}_2\text{M}((\text{PR})_2)$ and $\text{Cp}_2\text{M}((\text{PR})_3)$ Complexes†

Jianwei Ho, Tricia L. Breen, Andrzej Ozarowski, and Douglas W. Stephan*

Department of Chemistry and Biochemistry, University of Windsor, Windsor, Ontario, Canada N9B 3P4

Received August 6, 1993*

The compounds $\text{Cp}_2\text{M}((\text{PR})_3)$ ($\text{M} = \text{Zr}$, $\text{R} = \text{Ph}$ (**1**), Cy (**2**); $\text{M} = \text{Hf}$, $\text{R} = \text{Cy}$ (**3**)) and $\text{Cp}^*\text{Zr}((\text{PCy})_3)$ (**4**) were prepared and characterized. These compounds were prepared by the known reactions of the metallocene dihalide with primary phosphide salts. Alternatively, activation of the P–H bonds of a primary phosphine by zirconocene yields **1**, **2**, and **4**, respectively. Both stabilized metallocene(II) $\text{Cp}_2\text{Zr}(\text{SMe}_2)_2$ and metallocene generated by *in situ* reduction were employed. Attempts to identify intermediates in these reactions have been undertaken. Reaction of Cp_2ZrCl_2 with the phosphide LiPPh in the presence of NEt_4Br affords the species $[\text{Cp}_2\text{ZrBr}((\text{PPh})_2)]^+[\text{NEt}_4]^-$ (**5**). These results suggest a mechanism of formation of the $\text{M}(\text{PR})_3$ derivatives involving phosphinidene $\text{M}=\text{PR}$ and $\text{M}((\text{PR})_2)$ intermediates. Intervention in such a mechanism is also accomplished by the additional electron on $\text{V}(\text{IV})$. Thus reaction of Cp_2V with PH_2Ph yields $\text{Cp}_2\text{V}((\text{PPh})_2)$ (**6**). Although this reaction could not be halted at the intermediate phosphinidene, species **6** was also generated via the reaction of Cp_2VMeCl with LiPPh . In a similar reaction $\text{Cp}_2\text{V}(\text{PC}_6\text{H}_2\text{-2,4,6-Me}_3)_2$ (**7**) was generated in the reaction of Cp_2V with $\text{PH}_2(\text{C}_6\text{H}_2\text{-2,4,6-Me}_3)$. In contrast, reaction of the species $[\text{Cp}_2\text{V}]^+$ with PH_2Ph led only to the formation of the 18-electron product $[\text{Cp}_2\text{V}(\text{PH}_2\text{Ph})_2]^+$ (**8**). These results are described, and the implications of these results with particular reference to the mechanism of P–P bond formation are considered. Compounds **1**, **2**, **4–6**, and **8** were characterized crystallographically. Compound **1** crystallizes in space group $P2_1/a$ with $a = 8.159(5)$ Å, $b = 36.838(22)$ Å, $c = 8.338(5)$ Å, $\beta = 100.09(6)^\circ$, $V = 2467(3)$ Å³, and $Z = 4$. Compound **2** crystallizes in space group $P2_1/n$ with $a = 13.022(8)$ Å, $b = 9.303(9)$ Å, $c = 23.127(10)$ Å, $\beta = 93.25(5)^\circ$, $V = 2797(3)$ Å³, and $Z = 4$. Compound **4** crystallizes in space group, $I4/m$ with $a = 22.900(16)$ Å, $c = 14.975(8)$ Å, $V = 7853(5)$ Å³, and $Z = 16$. Compound **5** crystallizes in space group $P\bar{1}$ with $a = 11.557(3)$ Å, $b = 12.455(5)$ Å, $c = 11.527(4)$ Å, $\alpha = 93.44(3)^\circ$, $\beta = 91.25(3)^\circ$, $\gamma = 62.52(2)^\circ$, $V = 1469(2)$ Å³, and $Z = 2$. Compound **6** crystallizes in space group $P2_1/n$ with $a = 15.399(2)$ Å, $b = 19.876(5)$ Å, $c = 6.2129(9)$ Å, $\beta = 90.02(1)^\circ$, $V = 1901.5(5)$ Å³, and $Z = 4$. Compound **8** crystallizes in space group $P\bar{1}$ with $a = 11.103(3)$ Å, $b = 16.121(5)$ Å, $c = 10.895(4)$ Å, $\alpha = 94.63(3)^\circ$, $\beta = 105.96(2)^\circ$, $\gamma = 98.04(2)^\circ$, $V = 1842(1)$ Å³, and $Z = 2$.

Introduction

A subset of early metal–phosphorus derivatives is the group of complexes which also contain P–P bonds. The first such species prepared was the triphosphanato complex $\text{Cp}_2\text{Zr}((\text{PPh})_3)$, reported in 1972 by Issleib et al.¹ Subsequently, Kopf and Voigtlander² prepared and studied the solution properties of a series of related Ti, Zr, and Hf triphosphanato complexes. An X-ray crystallographic study of the species $\text{Cp}_2\text{Hf}((\text{PPh})_3)$ confirmed the planar nature of the HfP_3 core.³ In 1989, Benac and Jones⁴ described the preparation of phosphido, triphosphanato, and diphosphanato complexes via the reactions of various metallocene (Zr, Hf) dihalides with primary phosphides. Also in 1989, the tantalum diphosphanato complex $\text{Cp}_2\text{TaH}((\text{PPh})_2)$ ⁵ was prepared via the reaction of Cp_2TaH_3 and Ph_2PH although the mechanism of formation was not clear. More recently, we demonstrated that Zr bis(phosphides) of the form $\text{Cp}^*\text{Zr}(\text{PHR})_2$ lose PRH_2 to give terminal Zr phosphinidene ($\text{Zr}=\text{PR}$) intermediates.^{6,7} Reaction of the phosphinidene with the liberated phosphine in the opposing regiochemistry affords diphosphanato $\text{Cp}^*\text{Zr}((\text{PR})_2)$ ($\text{R} = \text{C}_6\text{H}_2\text{Me}_3$) and triphosphanato $\text{Cp}_2\text{Zr}((\text{PR})_3)$ ($\text{R} = \text{Ph}$) complexes. Although the reactivity of these P_1 , P_2 , and P_3 systems with organic substrates continues to be a

fruitful area of research,⁷ the nature of the reactions from which P–P bonds are derived continues to be of interest. In this report, we describe the synthesis of related Zr(IV), Hf(IV), and V(IV) phosphanato systems. These respective diamagnetic and paramagnetic systems provide insight into the process of P–P bond formation. Spectroscopic and structural data are presented to support the proposition of a mechanism while the implications of these results are considered.

Experimental Section

General Data. All preparations were done under an atmosphere of dry, O_2 -free N_2 employing either Schlenk line techniques or a Vacuum Atmospheres inert-atmosphere glovebox equipped with a catalyst column and an atmosphere circulation system. Solvents were reagent grade, distilled from the appropriate drying agents under N_2 and degassed by the freeze–thaw method at least three times prior to use. ^1H and $^{13}\text{C}\{^1\text{H}\}$ NMR spectra were recorded on Bruker AC-300 and AC-200 spectrometers operating at 300 and 200 MHz, respectively. Trace amounts of protonated solvents were used as references, and chemical shifts are reported relative to SiMe_4 . ^{31}P and $^{31}\text{P}\{^1\text{H}\}$ NMR spectra were recorded on a Bruker AC-200 operating at 81 MHz, and chemical shifts are reported to 85% H_3PO_4 . X-band EPR spectra were recorded on a Bruker EPS-300e EPR spectrometer equipped with a nuclear magnetometer and an HP frequency counter. Simulation and manipulation of the EPR data were performed using the Bruker software package Simfonia, which calculates Zeeman and hyperfine interactions up to the second order by the perturbation method. Nuclear quadrupole terms were neglected. Combustion analyses were performed by Galbraith Laboratories Inc., Knoxville, TN, and Schwarzkopf Laboratories, Woodside, NY. The primary phosphines were obtained from Quantum Design. Cp_2VCl_2 , Cp_2ZrCl_2 , PH_2Ph , PH_2Cy , and Cp^*ZrCl_2 were purchased from the Strem Chemical Co. or Pressure Chemical Co. Mg powder was purchased from the Aldrich Chemical Co. $\text{Li}(\text{PHR})(\text{THF})_x$ ⁷ and Cp_2VMeCl ⁸ were prepared by literature methods.

† In this paper boldface Arabic numbers designating species may refer to either an ionic coordination sphere or its neutral salt.

* Abstract published in *Advance ACS Abstracts*, February 1, 1994.

- Issleib, K.; Wille, G.; Krech, F. *Angew. Chem., Int. Ed. Engl.* **1972**, *11*, 527.
- Kopf, H.; Voigtlander, R. *Chem. Ber.* **1981**, *114*, 2731.
- Hey, E.; Bott, S. G.; Atwood, J. L. *Chem. Ber.* **1988**, *121*, 561.
- Benac, B. L.; Jones, R. A. *Polyhedron* **1989**, *8*, 1774.
- Leblanc, J. C.; Moise, C. *J. Organomet. Chem.* **1989**, *364*, C3.
- Hou, Z.; Stephan, D. W. *J. Am. Chem. Soc.* **1992**, *114*, 10088.
- Hou, Z.; Breen, T. L.; Stephan, D. W. *Organometallics* **1993**, *12*, 3158.

Table 1. Crystallographic Parameters

	1	2	3	4	6	8
formula	C ₂₈ H ₂₅ P ₃ Zr	C ₂₈ H ₂₃ P ₃ Zr	C ₃₅ H ₄₆ P ₁₃ Zr	C ₃₀ H ₄₀ P ₂ BrNZr	C ₂₂ H ₂₀ P ₂ V	C ₄₆ H ₄₄ BP ₂ V
a (Å)	8.159(5)	13.022(8)	22.900(16)	11.557(3)	15.399(2)	11.103(3)
b (Å)	36.838(22)	9.303(9)		12.455(5)	19.876(5)	16.121(5)
c (Å)	8.338(5)	23.127(11)	14.975(8)	11.537(4)	6.2129(9)	10.895(4)
α (deg)				93.44(3)		94.63(3)
β (deg)	100.09(6)	93.25(5)		91.25(3)	90.02(1)	105.96(2)
γ (deg)				62.52(2)		98.04(2)
space group	P2 ₁ /a (No. 14)	P2 ₁ /n (No. 14)	I4/m (No. 87)	P $\bar{1}$ (No. 2)	P2 ₁ /n (No. 14)	P $\bar{1}$ (No. 2)
V (Å ³)	2467(3)	2797(3)	7853(5)	1469.3(9)	1901.5(5)	1842(1)
D _{calcd} (g cm ⁻³)	1.40	1.34	1.22	1.46	1.39	1.30
Z	4	4	8	2	4	2
abs coeff, μ (cm ⁻¹)	6.51	5.79	4.27	18.66	6.71	3.34
T (°C)	24	24	24	24	24	24
R ^a (%)	7.21	8.96	8.92	7.50	7.53	5.82
R _w ^b (%)	5.66	6.03	7.58	6.02	5.64	3.96

$$^a R = \sum ||F_o| - |F_c|| / \sum |F_o|. \quad ^b R_w = [\sum (|F_o| - |F_c|)^2 / \sum |F_o|^2]^{0.5}.$$

Synthesis of Cp₂Zr(PR)₃ (R = Ph (1)¹, Cy (2)). These compounds can be prepared by several methods. One example of each of the various methods follows. (i) To 20 mL of a THF solution of Cp₂ZrCl₂ (146 mg, 0.5 mmol) was added excess Mg (powder). The mixture was stirred for 1 h, and then PH₂Ph (170 mg, 1.5 mmol) was added. The mixture was stirred overnight and allowed to stand for 1 week. Addition of hexane afforded orange-brown crystals of **1**. Yield: 25%. (ii) To 20 mL of a THF solution of Cp₂ZrCl₂ (146 mg, 0.5 mmol) was added LiPHR(THF)_x (1.5 mmol) or KPHR (R = Ph, Cy)⁹ (1.5 mmol). The mixture was stirred overnight and allowed to stand for 24 h. Addition of hexane afforded orange-brown crystals of **1**. Yield: 30%. Yield of **2**: 30%. (iii) To a THF solution of Cp₂Zr(SMe₂)₂¹⁰ (345 mg, 1.0 mmol) was added PH₂R (3.0 mmol). The mixture was stirred overnight and allowed to stand for 24 h. Addition of hexane afforded orange-brown crystals of **1**. Yield: 30%. Yield of **2**: 30%. (iv) To a toluene solution of CyPH₂ (116 mg, 1.0 mmol) was added BuLi (0.8 mL of 2.5 M, 2.0 mmol) at -78 °C. The solution was warmed to room temperature, and Cp₂ZrCl₂ (292 mg, 1.0 mmol) was added. The solution became dark immediately. After the solution was allowed to stand for several days, a small portion of hexane was added, which resulted in the deposition of brown crystals of **2**. Yield: 25%. Experimental data for **1** are as follows. ¹H NMR (C₆D₆, 25 °C) δ: 5.12 (s, Cp, 5H), 5.35 (t, Cp, 5H), 6.81–8.25 (m, br, Ph, 15H). ³¹P NMR (C₆D₆, 25 °C) δ: 89.1 (d, |J_{P-P}| = 349.9 Hz), -187.3 (t, |J_{P-P}| = 349.9 Hz).¹ Experimental data for **2** follow. ¹H NMR (C₆D₆, 25 °C) δ: 5.56 (s, Cp, 5H), 5.45 (t, Cp, 5H), 1.83, 1.77, 1.57 (br, Cy, 33H). ³¹P NMR (C₆D₆, 25 °C) δ: 126.0 (d, |J_{P-P}| = 346.0 Hz), -182.5 (t, |J_{P-P}| = 346.0 Hz). Anal. Calcd: C, 59.50; H, 7.50.

Synthesis of Cp₂Hf(PCy)₃ (3). Excess KPHCy (231 mg, 1.5 mmol) was added to a suspension of Cp₂HfCl₂ (190 mg, 0.5 mmol) in THF. The solution became brown and was stirred overnight. The solution was filtered, and the volume of the filtrate was reduced. The resulting solution was again filtered, and hexane was added, yielding yellow-orange crystals of **3**. Yield: 30%. ¹H NMR (C₆D₆, 25 °C) δ: 5.52 (s, Cp, 5H), 5.41 (t, Cp, 5H), 1.85, 1.76, 1.70 (m, br, Cy, 33H). ³¹P NMR (THF, 25 °C) δ: 88.1 (d, |J_{P-P}| = 319.4 Hz), -189.6 (t, |J_{P-P}| = 319.4 Hz). Anal. Calcd: C, 51.66; H, 6.66. Found: C, 51.44; H, 6.40.

Synthesis of Cp^{*}₂Zr(PCy)₃ (4). Cp^{*}₂ZrCl₂ (86 mg, 0.2 mmol) in THF (5 mL) was reacted with excess Mg (powder) at -78 °C for 5 h; then PH₂Cy (50 mg, 0.4 mmol) was added. A red-brown solution was immediately obtained which gradually became green over a week of standing. The solution was filtered, the filtrate volume was reduced, and hexane was added. This gave orange crystals of **4** upon several days of standing (30% yield). ¹H NMR (C₆D₆, 25 °C) δ: 1.84 (s, Cp^{*}, 15H), 1.51 (s, Cp^{*}, 15H), 1.89, 1.87, 1.82 (m, br, Cy, 33H). ³¹P NMR (C₆D₆, 25 °C) δ: 106.0 (d, |J_{P-P}| = 308.5 Hz), -146.2 (t, |J_{P-P}| = 308.5 Hz). Anal. Calcd: C, 64.83; H, 9.02. Found: C, 64.60; H, 8.88.

Synthesis of [Cp₂Zr((PPh)₂)Br][NEt₄] (5). To a THF solution of PH₂Ph (110 mg, 1.0 mmol) was added excess KH. This resulted in an orange solution. The solution was stirred for 1 h, and the excess KH was filtered off. Cp₂ZrCl₂ (145 mg, 0.5 mmol) was added to the filtrate together with excess Et₄NBr. The reaction mixture was stirred and filtered, and the volume of the filtrate was reduced. Hexane was added, affording red-orange crystals of **5**. Yield: 15%. ¹H NMR (CD₂Cl₂, 25 °C) δ: 7.28, 7.27 (m, Ph, 10H), 6.46 (s, Cp, 10H), 3.35 (q, CH₂, 8H), 1.15 (t, CH₃, 12H). ³¹P NMR (THF, 25 °C) δ: -48.5 (d, |J_{P-P}| = 294.0 Hz), -75.0 (d, |J_{P-P}| = 294.0 Hz). Anal. Calcd: C, 55.63; H, 6.22. Found: C, 55.40; H, 6.02.

Synthesis of Cp₂V((PPh)₂) (6). (i) To a solution of Cp₂V (100 mg, 0.55 mmol) in one of benzene, THF, or MeCN was added excess PH₂Ph (100 mg). The solution was allowed to stand for 48 h. In some cases, crystallization of the dark purple-black **6** was spontaneous; in others, this was induced by the addition of hexane. Yield: 75%. (ii) To a solution of Cp₂VMeCl (100 mg, 0.43 mmol) in benzene or THF was added LiPHPh-THF (81 mg, 0.43 mmol). The solution was allowed to stand for 48 h, and the reaction was monitored by EPR spectroscopy. Dark purple-black **6** crystallized from solution following the addition of hexane. Yield: 20%. EPR (C₆D₆, 25 °C): g_{iso} = 2.0033; ⟨a_{V_{iso}}⟩ = 44.6 × 10⁻⁴ cm⁻¹, ⟨a_{P_{iso}}⟩ = 4.9 × 10⁻⁴ cm⁻¹. EPR (C₆D₆, -196 °C) g_x = 1.9795, g_y = 1.9950, g_z = 2.0305; ⟨a_{V_x}⟩ = 68.7 × 10⁻⁴ cm⁻¹, ⟨a_{V_y}⟩ = 3.8 × 10⁻⁴ cm⁻¹, ⟨a_{V_z}⟩ = 68.9 × 10⁻⁴ cm⁻¹; ⟨a_{P_x}⟩ = 16.3 × 10⁻⁴ cm⁻¹, ⟨a_{P_y}⟩ = 0.8 × 10⁻⁴ cm⁻¹, ⟨a_{P_z}⟩ = 0.8 × 10⁻⁴ cm⁻¹. Anal. Calcd: C, 66.51; H, 5.07. Found: C, 66.38; H, 4.92.

Generation of Cp₂V((PC₆H₂-2,4,6-Me₃)₂) (7). (i) To a solution of Cp₂V (100 mg, 0.55 mmol) in one of benzene, THF, or MeCN was added excess PH₂(C₆H₂-2,4,6-Me₃) (100 mg). The solution was allowed to stand for 48 h, and the reaction was monitored by EPR. (ii) To a solution of Cp₂VMeCl (100 mg, 0.43 mmol) was added LiPH(C₆H₂-2,4,6-Me₃)-2THF (130 mg, 0.43 mmol), and the reaction was monitored by EPR. Attempts to crystallize or precipitate **7** from either reaction were unsuccessful. EPR (C₆D₆, 25 °C): g = 2.0041; ⟨a_{V_{iso}}⟩ = 45.7 × 10⁻⁴ cm⁻¹.

Synthesis of [Cp₂V(PH₂Ph)₂][BPh₄] (8). To a solution of Cp₂VCl (100 mg, 0.46 mmol) in 3 mL of THF were added excess PH₂Ph (100 mg) and NaBPh₄ (157 mg, 0.46 mmol). The solution was stirred overnight and filtered. To the filtrate was added 1 mL of hexane, and the mixture was allowed to stand for 48 h. This yielded crystals of **8** in 82% yield. Anal. Calcd: C, 76.68; H, 6.15. Found: C, 76.22; H, 5.98.

X-ray Data Collection and Reduction. X-ray-quality crystals were obtained directly from the preparations as described above. The crystals were manipulated and mounted in capillaries in a glovebox, thus maintaining a dry, O₂-free environment for each crystal. Diffraction experiments were performed on a Rigaku AFC6 diffractometer equipped with graphite-monochromatized Mo Kα radiation. The initial orientation matrices were obtained from 20 machine-centered reflections selected by an automated peak search routine. These data were used to determine the crystal systems. Automated Laue system check routines around each axis were consistent with the crystal systems reported in Table 1. Ultimately, 25 reflections (20° < 2θ < 25°) were used to obtain the final lattice parameters and the orientation matrices. Machine parameters, crystal data, and data collection parameters are summarized in Table 1. The observed extinctions were consistent with the space group given in Table 1. Where space group ambiguities were encountered, the space group assignments were confirmed by successful refinement. The data

(8) Razuvaev, G. A.; Bayuskin, P. Y.; Cherkasov, V. K.; Phokeev, A. P. *Inorg. Chim. Acta* **1980**, *44*, L103.

(9) This species was prepared via reaction of excess KH with PH₂R. Filtration and solvent removal afforded clean KPHR (by NMR) which was used as is.

(10) This compound was generated *in situ* by analogy to the preparation of Cp₂Zr(PMe₃)₂ with the substitution of SMe₂ for PMe₃. See: Kool, L. B.; Rausch, M. D.; Alt, H. G.; Herberhold, M.; Thewalt, U.; Honold, B. *J. Organomet. Chem.* **1986**, *310*, 27.

sets were collected in one shell ($4.5^\circ < 2\theta < 50.0^\circ$), and three standard reflections were recorded every 197 reflections. The intensities of the standards showed no statistically significant change over the duration of the data collection. Empirical absorption corrections were applied to each data set based on ψ -scan data. The data were processed using the TEXSAN crystal solution package operating on a VAX 3520 workstation. The reflections with $F_o^2 > 3\sigma(F_o^2)$ were used in the refinement.

Structure Solution and Refinement. Non-hydrogen atomic scattering factors were taken from the literature tabulations.¹¹⁻¹³ The Zr atom positions were determined using direct methods employing either the SHELX-86 or MITHRIL direct methods routines. In each case, the remaining non-hydrogen atoms were located from successive difference Fourier map calculations. The refinements were carried out by using full-matrix least-squares techniques on F_o , minimizing the function $w(|F_o| - |F_c|)^2$ where the weight w is defined as $4F_o^2/2\sigma(F_o^2)$ and F_o and F_c are the observed and calculated structure factor amplitudes. In the final cycles of refinement, all heavy atoms were assigned anisotropic temperature factors. The number of carbon atoms assigned anisotropic thermal parameters varied among the five structures and was set so as to maintain a reasonable data:variable ratio in each case. Hydrogen atom positions were calculated and the hydrogens were allowed to ride on the carbon to which they are bonded by assuming a C-H bond length of 0.95 Å. Hydrogen atom temperature factors were fixed at 1.10 times the isotropic temperature factor of the carbon atom to which they are bonded. In all cases, the hydrogen atom contributions were calculated but not refined. The final values of R and R_w are given in Table 1. The maximum Δ/σ for the parameters in the final cycles of the refinement are also given in Table 1. The residual electron densities were of no chemical significance. The following data for **1**, **2**, **4-6**, and **8** have been deposited as supplementary material: positional parameters, thermal parameters, selected bond distances and angles, and hydrogen atom parameters.

Results

Benac and Jones⁴ have previously described the synthesis of complexes of the form $Cp_2M((PPh)_3)$ ($M = Zr, Hf$) via the reaction of the metallocene dihalide with LiPPh. In a similar manner, the reaction of Cp_2MCl_2 with the appropriate primary lithium or potassium phosphides affords the species $Cp_2M((PR)_3)$ ($M = Zr, R = Ph$ (**1**), Cy (**2**); $M = Hf, R = Cy$ (**3**)). In addition to 1H NMR spectra which are consistent with these formulations, these complexes exhibit the characteristic $^{31}P\{^1H\}$ NMR resonances consisting of a low-field doublet and a high-field triplet. The chemical shift and coupling constant data are consistent with the trends in Lewis acidity of the metal centers.⁴

The $Zr((PR)_3)$ complexes are also accessible via reactions involving P-H activation by Zr(II). Reduction of Cp_2ZrCl_2 or $Cp^*_2ZrCl_2$ by Mg followed by subsequent addition of phosphine yields **1** and **4** although the respective yields are moderate. The inefficiency of heterogeneous Mg reduction presumably accounts for the low yields. An alternative route for the generation of Cp_2Zr^{II} is the Negishi method¹⁴ employing BuLi. Subsequent generation of the zirconocene derivative $Cp_2Zr(SMe_2)_2$ and reaction with appropriate primary phosphine yields **1** and **2**, respectively. Alternatively in situ generation of $Cp^*_2Zr^{II}$ and subsequent addition of PH_2Cy afford **4**. These synthetic routes to **1** and **2** are not clean, as other products including Zr(III) phosphide dimers are isolable from these reactions with minor perturbations to the reaction conditions.¹⁵ This suggests that several pathways are available for the initial intermediates formed in these reactions.

The course of the above reactions leading to the $M((PR)_3)$ complexes has been investigated. Reaction of Cp_2ZrCl_2 with

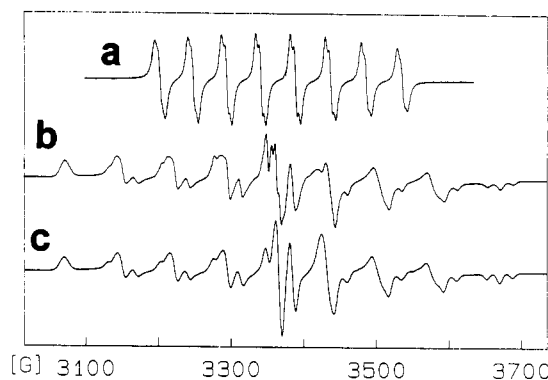


Figure 1. EPR spectra of (a) **6** in C_6H_6 solution and (b) **6** in frozen solution. Trace c is the simulated frozen-solution spectrum of **6**.

KPHPh in the presence of NEt_4Br did prevent the formation of **1** to some extent. While the majority of the product (70%) was unchanged (i.e. **1**), a second product was formed in about 30% yield (by NMR). This product exhibited a pair of coupled doublets in the ^{31}P NMR spectrum at -48.5 and -75.0 ppm. Subsequent isolation and characterization suggested this new species was $[Cp_2Zr((PPh)_2)Br][NEt_4]$ (**5**). This formulation was confirmed crystallographically (vide infra). The ^{31}P NMR chemical shifts observed for **5** are in marked contrast to those observed for $Cp^*_2Zr((PC_6H_2Me_3)_2)$ (131.0 ppm)⁷ and other such $((PR)_2)$ complexes.¹⁶ This difference is attributable to greater electron density at the metal center in **5**, which is formally an 18-electron species. Subsequently, it was shown that addition of NEt_4Br to a solution of **1** resulted in no reaction. This indicates that the formation of **5** arises from intervention of the bromide ion in the formation of **1**.

Reaction of PH_2Ph with Cp_2V proceeds to yield a dark solution which upon addition of hexane yields a black paramagnetic crystalline solid **6**. This product exhibits an eight-line EPR spectral typical of V(IV) complexes with an $\langle a_{V_{iso}} \rangle$ value of $44.6 \times 10^{-4} cm^{-1}$. Some additional superhyperfine coupling is evident in the spectrum (Figure 1a). This small coupling is attributed to an $\langle a_{P_{iso}} \rangle$ value of $4.9 \times 10^{-4} cm^{-1}$. The formulation of **6** was determined crystallographically to be $Cp_2V(PPh)_2$ (vide infra). In a similar fashion, reaction of $PH_2(C_6H_2-2,4,6-Me_3)$ with Cp_2V generates the V(IV) species formulated as $Cp_2V((PC_6H_2-2,4,6-Me_3)_2)$ (**7**) on the basis of the EPR data although, in this case, hyperfine coupling to P was not resolved. Compound **6** is also derived from the reaction of Cp_2VMeCl with LiPPh.

The frozen-solution EPR spectrum of **6** is shown in Figure 1b. Computer-generated spectral simulation shown in Figure 1c reveals estimated values of the anisotropy in g and $\langle a \rangle$. Previous dilute single-crystal EPR studies of Cp_2ML_2 ($M = Nb, V$)¹⁷⁻²⁰ showed that a smaller hyperfine component is directed in the plane bisecting the ML_2 angle. A similar anisotropy in $\langle a_V \rangle$ was also observed for the acetylene complexes $Cp_2V(RCCR)$,²⁰ which are structurally similar to **6**, consistent with the interpretation that the SOMO is an admixture of $3d_{z^2}/3d_{x^2-y^2}$. Occupation of this orbital, which is the $1a_1$ frontier orbital for the Cp_2M fragment,²¹ is also consistent with the anisotropy in the superhyperfine coupling to P observed for **6**.

While **6** and **7** are derived from the oxidative addition of P-H bonds to V(II), attempts to employ a similar method beginning with V(III) did not lead to V(V) species. Rather, reaction of $[Cp_2V][BPh_4]$ with PH_2Ph resulted in the formation of $[Cp_2V(PH_2Ph)_2][BPh_4]$ (**8**). Similar coordination complexes of

- (11) Cromer, D. T.; Mann, J. B. *Acta Crystallogr., Sect. A: Cryst. Phys., Diffraction, Theor. Gen. Crystallogr.* **1968**, *A24*, 324.
- (12) Cromer, D. T.; Mann, J. B. *Acta Crystallogr., Sect. A: Cryst. Phys., Diffraction, Theor. Gen. Crystallogr.* **1968**, *A24*, 390.
- (13) Cromer, D. T.; Waber, J. T. *International Tables for X-ray Crystallography*; Kynoch Press: Birmingham, England, 1974.
- (14) Negishi, E.; Cederbaum, F. E.; Takahashi, T. *Tetrahedron Lett.* **1986**, *Ho*, J.; Hou, Z.; Drake, R. J.; Stephan, D. W. *Organometallics* **1993**, *12*, 3145.

- (16) Weber, L. *Chem. Rev.* **1992**, *92*, 1839.
- (17) Petersen, J. L.; Dahl, L. F. *J. Am. Chem. Soc.* **1974**, *96*, 2248.
- (18) Petersen, J. L.; Dahl, L. F. *J. Am. Chem. Soc.* **1975**, *97*, 6116.
- (19) Petersen, J. L.; Dahl, L. F. *J. Am. Chem. Soc.* **1975**, *97*, 6422.
- (20) Petersen, J. L.; Griffith, L. *Inorg. Chem.* **1980**, *19*, 1852.
- (21) Hoffmann, R.; Lauher, J. J. *J. Am. Chem. Soc.* **1976**, *98*, 1729.

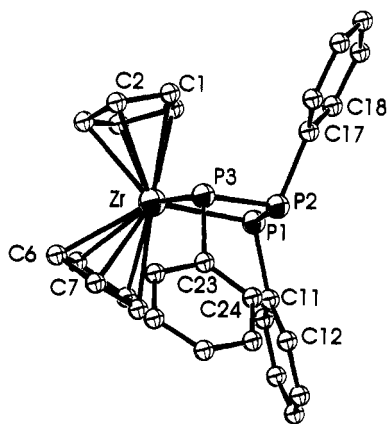


Figure 2. ORTEP drawing of **1**. 30% thermal ellipsoids are shown, and hydrogen atoms are omitted for clarity. Zr–P(1) = 2.631(5) Å, Zr–P(3) = 2.622(5) Å, P(1)–P(2) = 2.212(7) Å, P(2)–P(3) = 2.200(7) Å, and P(1)–Zr–P(3) = 89.8(2)°.

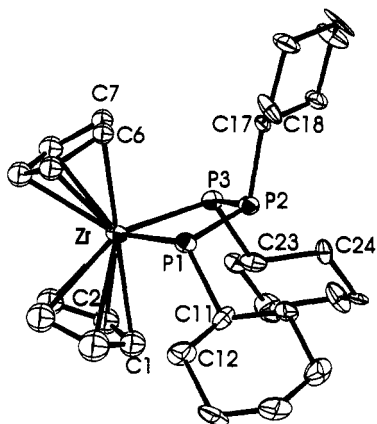
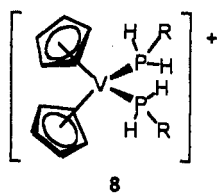


Figure 3. ORTEP drawing of **2**. 30% thermal ellipsoids are shown, and hydrogen atoms are omitted for clarity. Zr–P(1) = 2.621(6) Å, Zr–P(3) = 2.620(6) Å, P(1)–P(2) = 2.238(7) Å, P(2)–P(3) = 2.166(7) Å, and P(1)–Zr–P(3) = 90.4(2)°.

the form $[\text{Cp}_2\text{VLL}]^+\text{X}^-$ have been previously prepared but not structurally characterized.²² The structure of **8** was determined crystallographically.



Structural Studies

The structures of **1**, **2**, and **4** (Figures 2–4) are similar in that the coordination sphere of the Zr center in each is pseudotetrahedral composed of two Cp or Cp* ligands as well as two phosphorus atoms of the ((PR)₂) fragments. As was observed for Cp₂Hf((PPh)₃), the substituents on consecutive P atoms alternate sides of the ZrP₂ plane.³ These conformations minimize the substituent–substituent interactions. In the case of **4**, crystallographic symmetry dictates strict 2-fold molecular symmetry. The Zr–P distances average 2.627(6), 2.620(6), and 2.623(4) Å in **1**, **2**, and **4**, slightly longer than the Hf–P distance seen in Cp₂Hf((PPh)₃).³ These distances are significantly longer than the formal Zr–P double bond in Cp₂Zr(PC₆H₂-*t*-Bu)₃PM₃

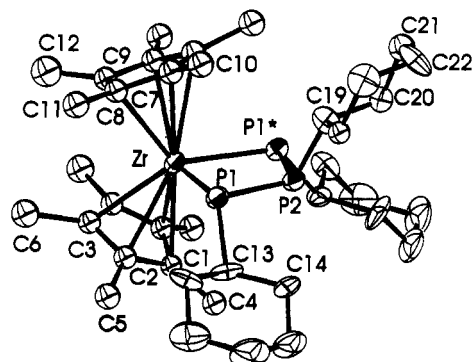


Figure 4. ORTEP drawing of **4**. 30% thermal ellipsoids are shown, and hydrogen atoms are omitted for clarity. Zr–P(1) = 2.623(4) Å, Zr–P(1); 2.623(4) Å, P(1)–P(2) = 2.181(5) Å, and P(1)–Zr–P(1)' = 87.7(2)°.

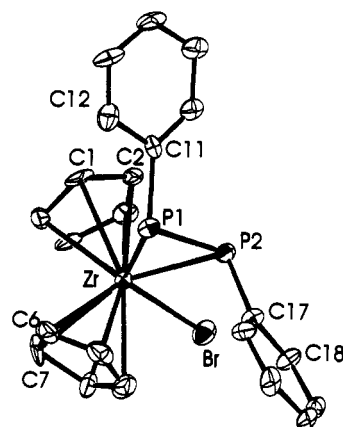


Figure 5. ORTEP drawing of the anion of **5**. 30% thermal ellipsoids are shown, and hydrogen atoms are omitted for clarity. Zr–P(1) = 2.745(5) Å, Zr–P(2) = 2.677(4) Å, Zr–Br = 2.813(3) Å, P(1)–P(2) = 2.145(6) Å, P(1)–Zr–P(2) = 46.6(1)°, P(1)–Zr–Br = 127.39(1)°, and P(2)–Zr–Br = 81.0(1)°.

(2.505(4) Å) and comparable to the Zr–P single bonds in Cp*₂Zr(PH(C₆H₂Me₃))₂ (2.63(2) Å), Cp*₂Zr(PH(C₆H₂Me₂CH₂)) (2.648(2) Å), and Cp*₂Zr((PC₆H₂Me₃)₂) (2.650(3) Å).⁷ The P–P bonds in **1**, **2**, and **4** vary from averages of 2.206(7), 2.203(7), and 2.18(5) Å, respectively. Each P atom adopts a distorted pyramidal geometry. In the case of the P atoms adjacent to Zr, the substituents are canted away from the metal center. For example, in **1** the Zr–P(1)–C(11) angle is 113.7(6)°, while the P(2)–P(1)–C(11) angle is 103.4(6)°. The substituent on the central P atom of the P₃ moieties is more symmetrically disposed (e.g. in **1**, P(1)–P(2)–C(17) = 102.0(6)° and P(3)–P(2)–C(17) = 102.4(6)°). The P–Zr–P angles in **1** and **2**, 89.8(2) and 90.4(2)°, respectively, are larger than that seen in **4** (87.7(2)°), reflecting the steric demands of the Cp* ligands.

The Zr atom in the anion of **5** is bonded to two Cp ligands, two P atoms, and a bromine atom (Figure 5). This geometry about Zr can also be described as pseudotetrahedral if one considers the (PR)₂ moiety as filling only one coordination site. The ZrP₂Br core is essentially planar, with the maximum deviation from the least-squares plane being 0.105(5) Å. The Zr–P distances in **5** are 2.745(5) and 2.677(4) Å, reflecting the chemical inequivalence of the two P environments in the anion. These Zr–P distances are longer than those seen in the related 16-electron compound Cp*₂Zr((PC₆H₂Me₃)₂) (2.650(3) Å)⁷, consistent with the 18-electron count about Zr in the anion of **5**. The shorter Zr–P(2) distance in **5** suggests a significant overlap of the P σ orbital with the 1a₁ frontier orbital of the Cp₂Zr fragment.²¹ The P–P distance is 2.145(6) Å. These data suggest weaker Zr–P bonds and a stronger P–P bond in **5** compared to those in

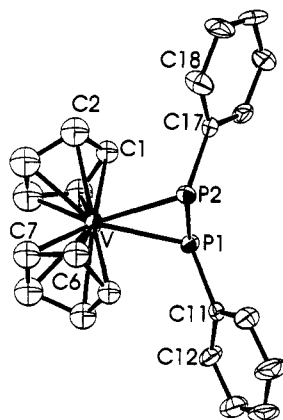


Figure 6. ORTEP drawing of **6**. 30% thermal ellipsoids are shown, and hydrogen atoms are omitted for clarity. V-P(1) = 2.538(4) Å, V-P(2) = 2.541(4) Å, P(1)-P(2) = 2.160(5) Å, and P(1)-V-P(2) = 50.3(1)°.

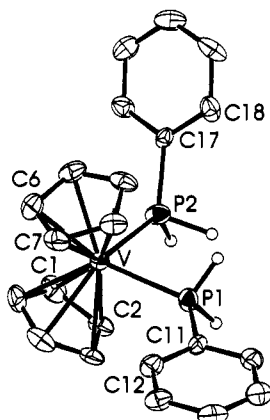
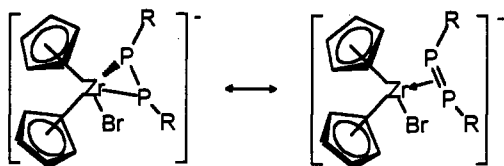


Figure 7. ORTEP drawing of **8**. 30% thermal ellipsoids are shown, and hydrogen atoms are omitted for clarity. V-P(1) = 2.391(2) Å, V-P(2) = 2.418(2) Å, and P(1)-V-P(2) = 83.52(8)°.

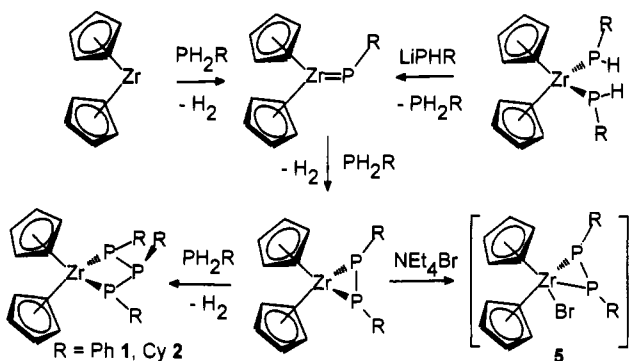
1, intimating contributions from the two resonance forms of the anion of **5**:



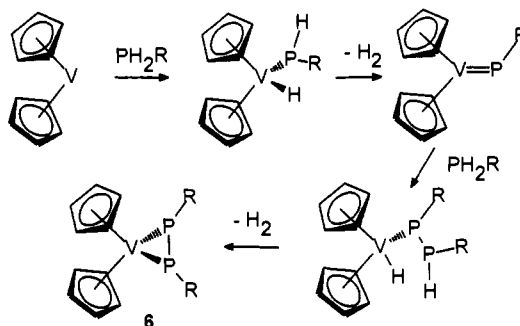
A similar description has been suggested for $\text{Cp}_2\text{TaH}(\text{PPh})_2$.⁵ Nonetheless, the Zr-P-C angles in **5** are 115.8(5) and 109.2(5)° for P(1) and P(2), respectively, while the P-P-C angles are 102.6(5) and 103.0(5)°. Further, the C-P-P-C dihedral angle is 141.3(9)°. These data are consistent with a distorted pyramidal geometry at P with the substituent on P(1) canted slightly away from the proximal cyclopentadienyl ring. These data suggest that **5** is most appropriately described as a metallacycle rather than a diphosphene complex.

The structures of **6** and the cation of **8** are structurally similar (Figures 6 and 7). In both cases, the pseudotetrahedral coordination spheres of V are composed of two Cp ligands and two P atoms. In the case of the neutral V(IV) species **6**, the P atoms are bonded, forming a three-membered ring, whereas in the V(III) cation **8** the P atoms are derived from two coordinated PH_2Ph ligands. The V-P distances average 2.539(4) and 2.404(4) Å for **6** and **8**, respectively. The shorter V-P distances in **8** are consistent with its cationic nature. The P-V-P angle in **8** is 83.52(8)°, typical of disubstituted metallocenes. In contrast, the corresponding angle in **6** is 50.3(1)°, typical of such MP_2 three-membered rings.

Scheme 1



Scheme 2



Discussion

In an earlier report,²³ we described monitoring the reactions of $\text{Cp}^*_2\text{ZrCl}_2$ with Mg and PH_2Cy by $^{31}\text{P}\{^1\text{H}\}$ and ^{31}P NMR spectroscopy. In that case, a resonance at 220.2 ppm was observed together with the resonance attributable to PH_2Cy . Here we report that these resonances gradually diminish in intensity and are replaced with the resonances arising from **4**. Attempts to isolate and further characterize the intermediate species which gives the resonance at 220.2 ppm have been unsuccessful. The absence of P-H coupling and the single P environment suggests either a P_1 or P_2 species. A diphosphanato intermediate of the form $\text{Cp}^*_2\text{Zr}(\text{PCy})_2$ is possible. Although the ^{31}P chemical shifts of $\text{Cp}_2^*\text{Zr}(\text{PR})_2$ (R = Ph, $\text{C}_6\text{H}_2\text{Me}_3$) are known to be 60 and 135 ppm, respectively, the ^{31}P chemical shift for $\text{Cp}'_2\text{Zr}(\text{P-}t\text{-Bu})_2$ ($\text{Cp}' = \text{C}_5\text{H}_3(\text{SiMe}_3)_2$) is 270.6 ppm.⁴ We have previously suggested²³ that the 220.2 ppm resonance arises from a terminal phosphinidene species $\text{Cp}^*_2\text{Zr}=\text{PCy}$. If this is the case, then a bent geometry is unlikely as the ^{31}P chemical shift of the bent phosphinidene fragment in $\text{Cp}_2\text{Zr}(\text{PC}_6\text{H}_2\text{-}t\text{-Bu}_3)\text{-PMe}_3$ is 792 ppm.⁷ A linear phosphinidene intermediate is possible, as the only known species with such a linear, terminal phosphinidene fragment $\text{WCl}_2(\text{CO})(\text{PC}_6\text{H}_2\text{-}t\text{-Bu}_3)(\text{PMe}_3)_2$ exhibits a ^{31}P NMR resonance at 193 ppm.²⁴ Such an intermediate would be expected to be highly reactive, perhaps explaining our inability to isolate this compound. Monitoring the related reaction of Cp_2ZrCl_2 and LiPHCy by ^{31}P NMR spectroscopy revealed a strong singlet resonance which exhibited no P-H coupling at 567.7 ppm as well as a resonance attributable to free PH_2Cy . These resonances also gradually diminish in intensity and are replaced with the resonances arising from **2**. The chemical shift of the intermediate suggests a bridging phosphinidene intermediate of the form $\text{Cp}_2\text{Zr}(\text{PCy})(\text{Cl})\text{Li}(\text{THF})_2$ although, once again, attempts to isolate this species have been unsuccessful. These data together with our previous studies⁷ suggest the intermediacy of phosphinidene complexes en route to **1-5** (Scheme 1). A similar reaction mechanism may be operative in the case of vanadocene,

(23) Ho, J.; Stephan, D. W. *Organometallics* **1991**, *10*, 3001.

(24) Cowley, A. H.; Pellerin, B. J. *Am. Chem. Soc.* **1990**, *112*, 6734.

affording **6** and **7** (Scheme 2), although this was not confirmed spectroscopically. In the formation of $\text{Cp}'_2\text{Zr}((\text{P-}i\text{-Bu})_2)$ ($\text{Cp}' = \text{C}_5\text{H}_3(\text{SiMe}_3)_2$)⁴ and $\text{Cp}^*_2\text{Zr}((\text{PC}_6\text{H}_2\text{Me}_3)_2)$,⁷ steric factors preclude further reaction leading to triphosphanato derivatives. In the case of **5**–**7**, electronic factors inhibit further reaction. Coordination of the bromide anion to the Zr center of **5** renders the Zr center coordinatively saturated and thus unreactive. In the 17-electron species **6** and **7**, the unpaired electron on V inhibits further reaction, as this would require a 19-electron intermediate. In the case of the Lewis acidic V(III), the reaction observed is simply coordination of 2 equiv of phosphine, giving **8**. Clearly, the relative redox potentials of V(III) and P–H bonds are not favorable for P–H oxidative addition.

A related imido system, $\text{Cp}_2\text{Zr}=\text{NR}(\text{L})$, was prepared via elimination of methane from $\text{Cp}_2\text{ZrMe}(\text{NHR})$. In an attempt

to intercept a $\text{Cp}_2\text{V}=\text{PR}$ intermediate, the reaction of Cp_2VMeCl with the primary phosphide was undertaken. Despite the fact that the stoichiometry was carefully controlled, the isolated product was, once again, **6**. The mechanism of this reaction is not understood.

Acknowledgment. Support from the PRF, administered by the American Chemical Society, and the NSERC of Canada is acknowledged. The award of an NSERC of Canada Postgraduate Scholarship to T.L.B. is also gratefully acknowledged.

Supplementary Material Available: Tables of positional parameters, selected bond distances and angles, thermal parameters, and hydrogen atom parameters, as well as a table of crystallographic parameters (25 pages). Ordering information is given on any current masthead page.